1.6 THE EFFECT OF FLOW OVER COASTAL TOPOGRAPHY ON THE CHARACTER OF LOW-LEVEL OFFSHORE WIND MAXIMA ALONG THE CALIFORNIA COAST IN SUMMER

Patrick S. Cross *
U.S. Navy/Submarine Forces, United States Pacific Fleet, Pearl Harbor, Hawaii

Douglas K. Miller and Wendell A. Nuss
Naval Postgraduate School, Monterey, California

1. INTRODUCTION

The California coastal jet has been examined in several studies. It is a persistent feature of the summertime wind pattern from southern Oregon to Point Conception in southern California. It is a low-level feature brought about by the combination of subsidence on the eastern side of the North Pacific high and the juxtaposition of hot temperatures over land and a cool marine layer over upwelled waters of the California current. The core of the jet is typically located within the temperature inversion at the top of the marine layer, although varying degrees of downward coupling result in extensions of high winds to the surface.

A major emphasis of this study was on defining the structure of the jet along a large section of coastline, and relating these large-scale jet variations to changes in the synoptic surface pressure gradient. The results of that portion of the study are outlined briefly in the next section. This observational focus was followed with a mesoscale modeling effort aimed at examining the dynamics involved in the jet's behavior near significant variations in coastal orientation or topography. It is that portion that is the emphasis of this paper. Specifically, the interplay between supercritical expansion and flow over topography in determining the structure of the marine boundary layer in the lee of major coastal features is addressed. The model setup is described in Section 3, with model results and discussion in Sections 4 and 5.

2. OBSERVATIONAL RESULTS

An examination of data from NOAA moored buoys along the California coast during June 1996, together with data from shore stations along the coast and in the interior yielded a distinct relationship between the orientation of the coastal pressure gradient and the magnitude of coastal jet winds as measured at the buoys. For example, winds at Buoy 28, south-southwest of Point Sur (Fig. 1), exhibited maximum magnitudes when the downcoast pressure gradient was maximized. Conversely, during periods of maximum cross-coast pressure gradient, as measured between Buoy 28 and NAS Lemoore in California's Central Valley, offshore winds were at their weakest, although remaining in a direction roughly parallel to the coastline.

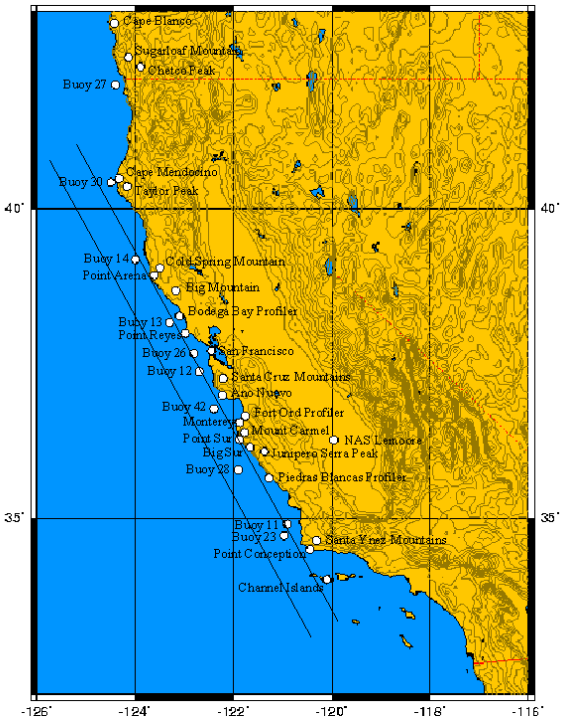

Figure 1. *The west coast of the United States, showing key locations and cross-sections discussed in the text.*

Synoptic sea-level pressure analyses from this time period indicate a pattern consistent with these observations. That is, when surface isobars near the coast are aligned approximately parallel to the coast, the cross-coast pressure gradient is maximized and offshore winds are reduced. Maximum offshore winds occur when there exists

Corresponding author address: Patrick S. Cross, U.S. Navy, Submarine Forces, U.S. Pacific Fleet, Pearl Harbor, Hawaii 96860; e-mail: crossps@csp.navy.mil.

a significant downcoast component of the pressure gradient (when the isobars become oriented more north-south, instead of parallel to the northwest to southeast oriented coastline). This pressure gradient reorientation appears to be largely driven by changes in the configuration of the interior thermal low.

Although this modulation of coastal jet wind speeds due to reorientation of the coastal pressure gradient occurs, it is important to note that the roughly coast-parallel direction of low-level winds persists throughout the vast majority of summer days. Above the marine layer, there is somewhat greater directional variability. Plots of buoy wind time series and NOGAPS analyses are contained in Cross (2003).

3. MODELING METHODOLOGY

A mesoscale model was employed in order to examine the interaction of these consistently northwesterly winds above and below the coastal marine layer with the topography near the coast. The model selected for this purpose was the Naval Research Lab Coupled Ocean Atmosphere Mesoscale Prediction System (COAMPS), as described in Hodur (1997). The model domain consisted of three nests with resolutions of 81, 27, and 9 km, as shown in Fig. 2. There were 45 vertical levels, with highest vertical resolution (40 m, increasing to 100 m) in the lower 1500 m of the atmosphere. Model top was set at 19,000 m.

Simulations were initialized at 0000 UTC on 9, 14, and 17 June 1996. Each simulation consisted of a 36-hour model run, initialized from a three-dimensional multiquadric (3DMQ) analysis of available observations blended with Navy Operational Global Atmospheric Prediction System (NOGAPS) analyses. The 3DMQ technique is derived from the two-dimensional version described in Nuss and Titley (1994), and identifies mathematically critical points in the dataset in three dimensions. Boundary conditions on the outer domain were constrained by subsequent NOGAPS analyses every twelve hours. This setup is essentially a cold start, in which mesoscale structure is allowed to establish itself in response to topographic and thermal forcing, without outer domain errors reaching into the inner domain of interest.

4. MODELING RESULTS

An extensive model validation is presented in Cross (2003). The structure of the marine boundary layer and coastal jet produced in COAMPS are shown to be consistent with a range of observations made during the CODE studies of the early 1980's off northern California, aircraft data collected during Coastal Waves 1996 near Cape Mendocino and Point Sur, and aircraft data from Parish (2000) off San Francisco. Further, the larger scale patterns are quite consistent with NOGAPS analyses, and wind speed variations from day to day at a given location agree well with the patterns observed at the NOAA buoys. The model is thus in reasonable agreement with the body of data available on the California summertime marine boundary layer and coastal jet. Thus, it is reasonable to utilize the more complete model fields to explore other aspects of the California coastal jet.

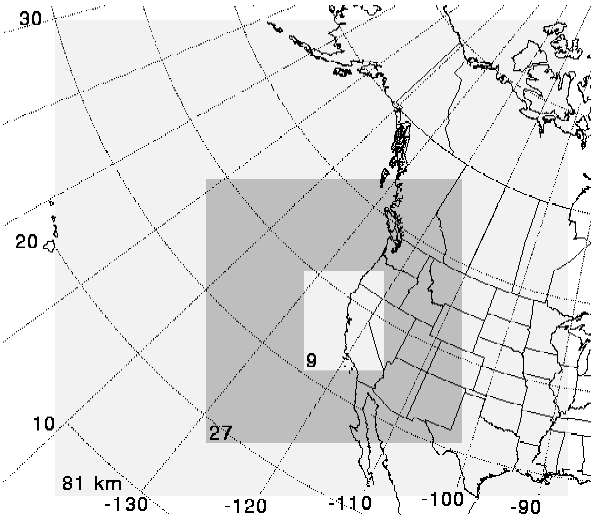

Figure 2. *COAMPS horizontal grid domains. Resolutions are shown in lower left of each grid.*

As seen in previous studies, the model consistently produces a well-mixed marine boundary layer capped by a strong thermal inversion. This inversion slopes downward from offshore toward the coast, with maximum slope close to the coast, and this slope is increased in the lee of significant coastal topography. Looking along the flow, which is nearly parallel to the coast, the model predicts sharp drops in isentropic surfaces in such lee areas, especially near the coast. The spatial distribution of model-predicted winds consistently indicates areas of maximum winds in the lee of coastal prominences, with weaker wind areas upstream and very close to the coast well downstream. These wind maxima are evident at the surface, but reach their vertical peak aloft, within the strong potential temperature gradient. Model winds undergo a diurnal cycle that is associated with varying scales of heating

over land areas, and that tends to produce maximum offshore winds and most shallow marine boundary layer depths in the late afternoon and early evening.

4.1 *Spatial Distribution of Winds*

An 850 mb ridge typically extends northeastward across the coast from the North Pacific high during summer. A clear relationship exists between the position of the axis of this ridge relative to the coast and the relative position of coastal jet winds along the coast. The COAMPS 850 mb height patterns at 1900 PDT on 9 and 14 June, along with isotachs at 980 mb (a level representative of the jet core), are shown in Figs. 3 and 4, respectively. Isotachs are shaded above 12 m s^{-1} to represent the approximate lateral extent of the coastal jet. When the ridge crosses the coast near the Oregon/California border, as in Fig. 3, the inception of jet winds is near Cape Mendocino and maximum winds are located to the south near Point Sur in central California. However, as seen in Fig. 4, when the ridge is displaced to the north such that it crosses the coast in southern Washington, coastal jet winds (and a jet structure in cross-section, as will be seen later) begin in southern Oregon, reach their maximum values in northern California, and are relatively weak further south. Evident in both plots is the large offshore extent of jet winds, with the 12 m s^{-1} threshold (direction remains generally coast-parallel) met up to 500 km offshore.

Also evident in Figs. 3 and 4 as different shades in the isotach pattern are regions of higher winds near the coast. These wind maxima occur near changes in coastal orientation, but also in a consistent direction from a nearby coastal mountain. Shown in Fig. 5 are 1000 mb isotachs from 14 June, shaded above 18 m s^{-1} to indicate regions of highest winds, with terrain higher than 400 m also shaded. High low-level wind areas are evident to the south of the southern Oregon coastal mountains, Taylor Peak (Cape Mendocino) and Big Mountain near Point Arena (locations in Fig. 1). A vector drawn from the coastal mountain to the wind maximum in each case is very closely aligned with the direction of flow above the marine layer at 850 mb. A less consistent spatial relationship exists between nearby coastal bends and their associated wind maxima. Further south, the small higher wind area near Point Sur is oriented more to the southwest of nearby Mount Carmel. This difference is attributable to the much weaker 850 mb winds to the south on 14 June. On 9 June (shown later), weak winds aloft at

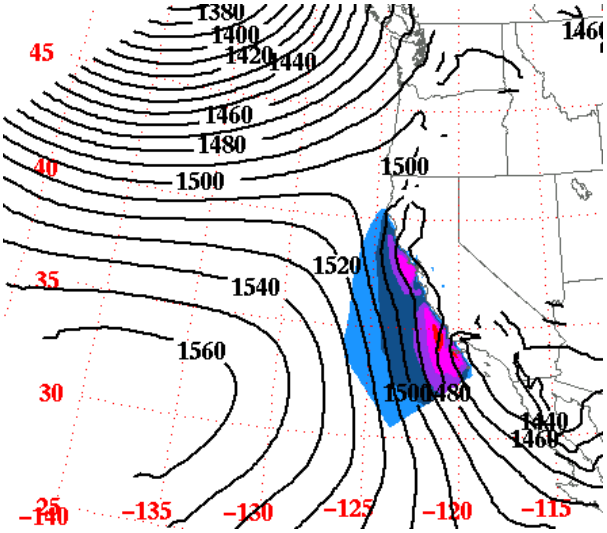

Figure 3. *COAMPS 850 mb heights (m, 10-m interval) from the 27-km nest, with isotachs at 980 mb (shaded above 12 m s^{-1}) from the 9-km nest, valid at 1900 PDT on 9 June 1996. Straight edges of 12 m s^{-1} winds indicate the limit of the 9-km nest.*

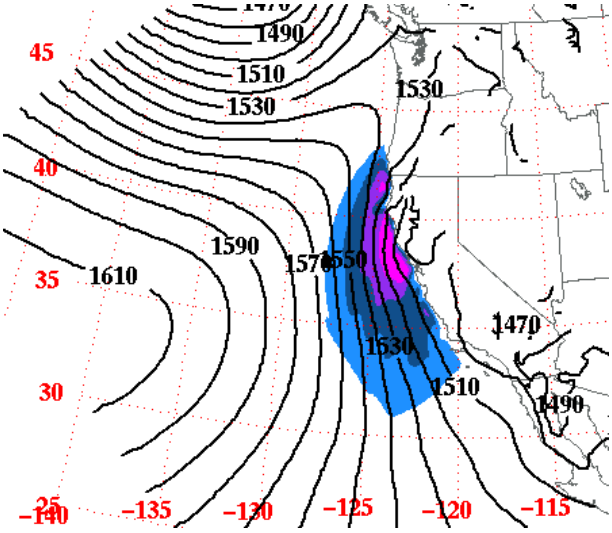

Figure 4. *As in Fig. 3, except from 14 June.*

Chetco Peak in southern Oregon result in a similarly localized offshore wind feature close to the coastal bend, while stronger winds over the terrain near Point Sur produce a broader low-level wind feature whose location is well aligned with the flow aloft.

Also evident in Fig. 5 are relatively weak 1000 mb wind areas on the upstream side of each coastal mountain. The existence of these minima is as prevalent a feature of the coastal wind distribution as the downwind maxima. They occur as flow in and above the marine layer impinges

upon the high terrain, causing a deepening of the marine layer and rise in surface pressures on the upwind side.

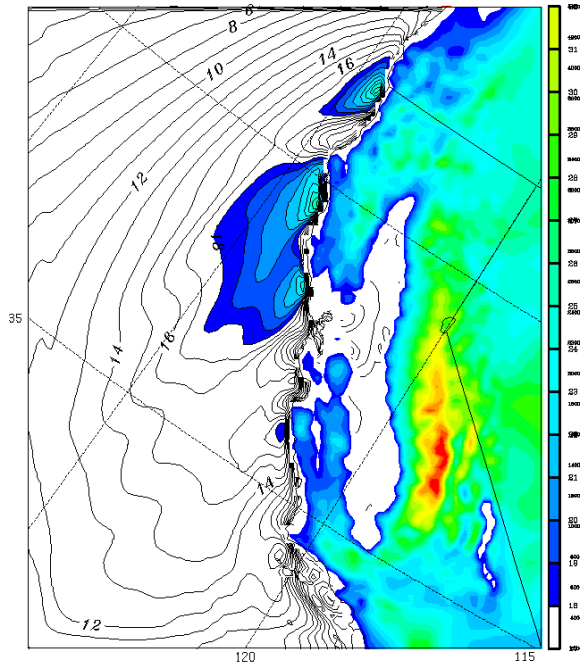

Figure 5. *1000 mb isotachs (m s^{-1}) from COAMPS valid at 1700 PDT 14 June 1996, with color shading above 18 m s^{-1} to highlight areas of highest winds along the coast. Also shown are terrain heights above 400 m (200-m interval).*

4.2 Cross-coast Structure

In cross-sections roughly perpendicular to the flow, and to the coast, a narrow, shallow jet in the north each day broadens to the south and quickly expands to heights of 1500 m or more, providing further evidence that the jet is a much larger feature than discussed in previous studies, and extends to heights much greater than the depth of the marine layer. This suggests the inadequacy of the depiction of the coastal jet as existing in a supercritical channel.

Important differences are seen in cross-sections drawn at varying positions relative to one of the six areas where significant mountains are in close proximity to the coast. A section upstream from one of the coastal mountain obstructions, as in Fig. 6 from the north side of Cape Mendocino, exhibits nearshore isentropes that slope upward toward the coast, as the flow impinges on the terrain and deepens the marine layer. Higher winds are evident up the face of the terrain as the flow accelerates around it. A section crossing the coast at or near a coastal mountain clearly shows an area of higher winds flowing over the terrain, as in Fig. 7 near Point Arena. Fig. 8 is an example of a cross-section in the close lee of a coastal mountain (Mount Carmel, near Point Sur). Here a steep downward isentropic slope is evident, associated with a compressed marine layer.

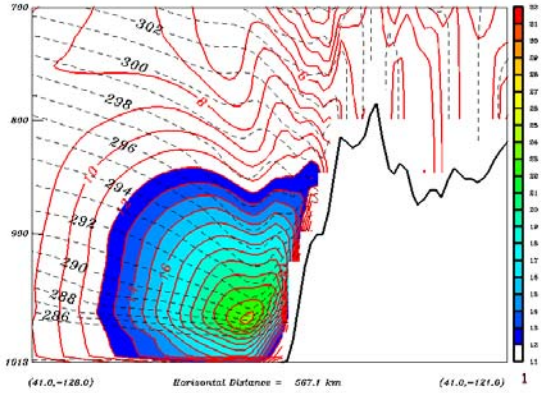

Figure 6. *East-west cross-section from COAMPS, valid at 1900 PDT 14 June 1996, of winds (solid lines, 1 m s^{-1} contour interval, shading above 12 m s^{-1}) and potential temperatures (dashed lines, 1 K contour interval) along 41°N.*

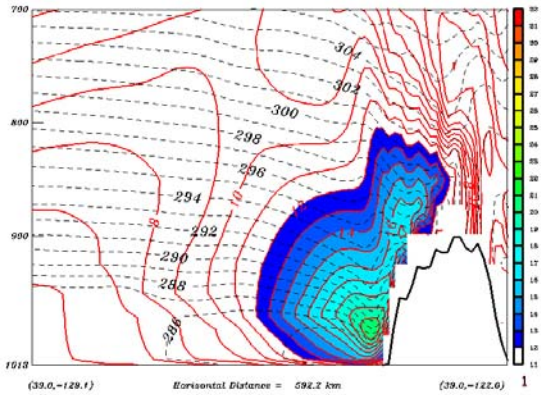

Figure 7. *As in Fig. 6, except valid at 1900 PDT 9 June 1996 and section along 39°N.*

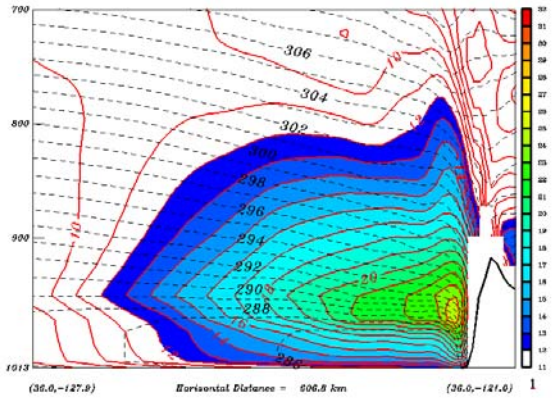

Figure 8. *As in Fig. 7, except section along 36°N.*

Finally, in Fig. 9, a steep downward isentropic slope is evident offshore in response to the flow in the extended lee of Mount Carmel, while further inshore there is an upward slope associated with flow impingement on the Santa Ynez Mountains. Further south (not shown), a second steep downward slope occurs in the lee of these mountains. A similar double isentropic drop, with upslope between, is seen on 14 June along 38°N (not shown), due to responses to both the Cape Mendocino and Point Arena terrain.

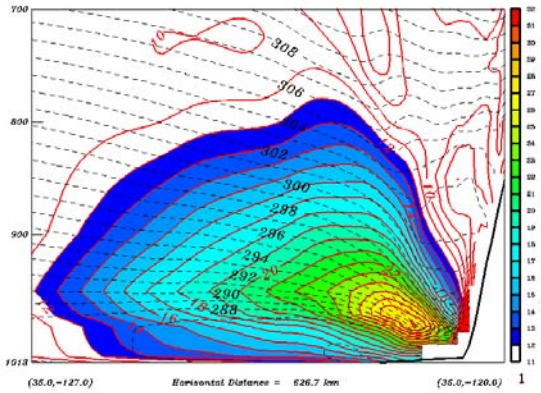

Figure 9. *As in Fig. 7, except section along 35°N.*

4.3 Along-coast Structure

Cross-sections from 14 June drawn parallel to the coast, as shown in Fig. 1, reveal important characteristics in the direction of flow. The stronger winds in the north on that day are apparent. On the nearshore section (Fig. 10),

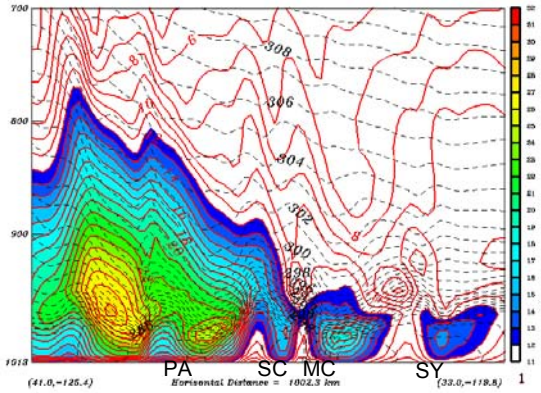

Figure 10. *Near-shore along-coast cross-section from COAMPS valid at 1900 PDT on 14 June 1996. Note the approximate along-coast locations of Point Arena (PA), the Santa Cruz Mountains (SC), Mount Carmel (MC), and the Santa Ynez Mountains (SY).*

distinct weak wind areas on the upstream side of each coastal obstruction and relative wind maxima downwind are evident. Isentropes slope up approaching each obstruction, and then sharply down on the lee side, resulting in a compressed marine layer and higher surface wind speeds. Also of note are the height to which increased winds are seen in the north, the relatively shallow extent of the higher wind areas in the south, and the upstream tilt of higher wind and isentropic

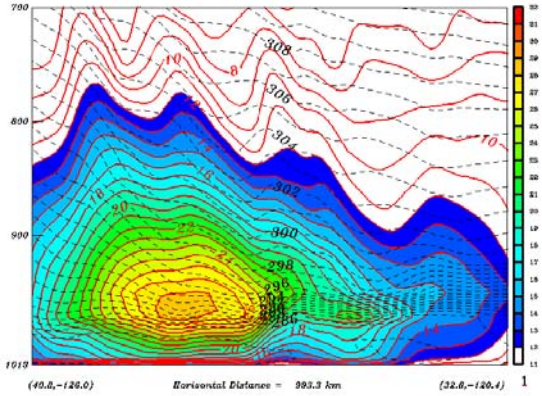

Figure 11. *As in Fig. 10, except section is 50 km farther offshore, as shown in Fig. 1.*

slope regions above the marine layer. The offshore section (Fig. 11), located 50 km farther from land, still exhibits a series of isentropic descents with a leveling off between each. Thus, even at this distance from shore, the effects of flow over and down the lee side of coastal topography can be seen. In fact, periodic steepening of isentropic surfaces to the south can be traced back to interaction with topography out to some 200 km from shore in some cases.

5. DISCUSSION

The presence of accelerated flow over terrain well above the marine layer, combined with the upstream tilt mentioned previously, are suggestive of mountain waves. Fig. 12 is a cross-section drawn from the terrain near Cape Blanco across Taylor Peak (Cape Mendocino). The isentropes over Taylor Peak show a pattern quite consistent with classic mountain wave theory (Durran, 1984) to a height of about 700 mb. The wave damping above that is attributed to both speed and directional shear in the winds above that level. While this is a particularly good example, similar upstream tilted wave patterns are seen in the flow over each coastal mountain whenever winds above the boundary layer are sufficiently strong

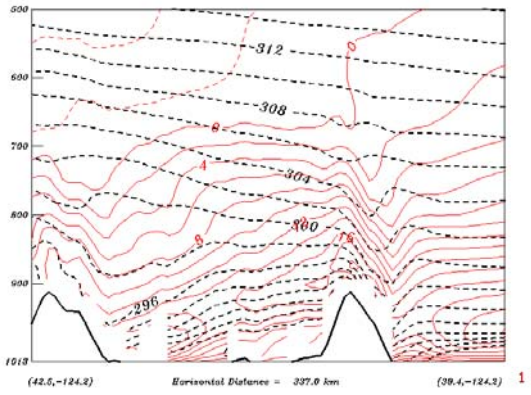

Figure 12. *Along-coast cross-section of scalar tangent winds (solid, m s^{-1}, 2 m s^{-1} contour interval) and potential temperatures (dashed, K, 2K contour interval) beginning in southern Oregon, crossing over water off northern California, and crossing Cape Mendocino near Taylor Peak. Section is valid at 1900 PDT 14 June 1996.*

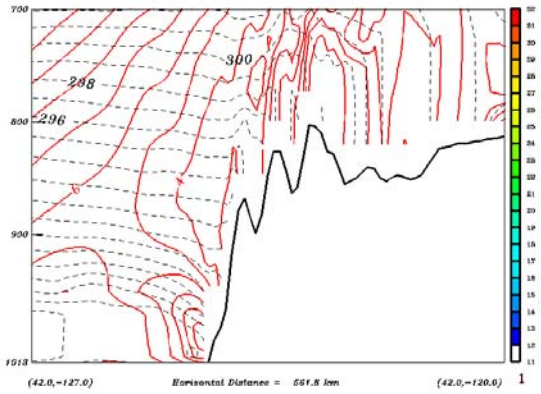

Figure 13. *As in Fig. 7 from 9 June, except section along 42°N.*

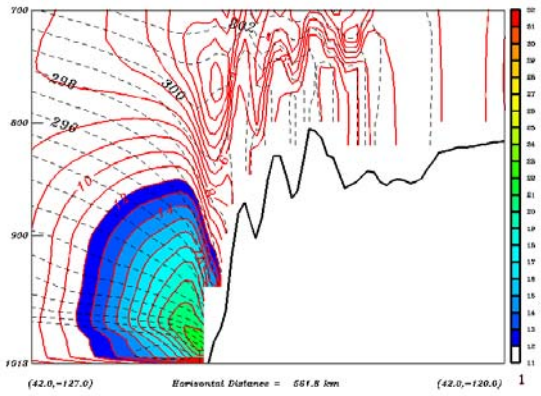

Figure 14. *As in Fig. 13, except from 14 June.*

(as in the south on 9 June and the north on 14 June).

The presence of these waves and their impact on the low-level wind pattern offshore and downstream bring into question the traditional explanation of these lee wind maxima as being caused primarily by supercritical expansion fan effects. Figs. 13 and 14 are cross-sections through 42°N along the Oregon-California border, just south of the high terrain near Chetco Peak and the coastal bend at Cape Blanco, from 9 and 14 June, respectively. On 9 June when the flow at 850 mb was weak and onshore over the peak, only a localized 9 m s^{-1} coastal jet maximum is evident. When the flow aloft is strong and oriented down the coast, as in Fig. 14, a deep coastal jet is present with maximum winds reaching well over 20 m s^{-1}. This is seen in plan view in Figs. 15 and 16.

It thus appears that when winds above the coastal mountains are sufficiently strong, the extent of the downstream low-level maximum is governed by a combination of supercritical expansion within the marine layer and the mountain wave effect from above the layer. The wave serves to further compress the marine layer beyond that which occurs due to expansion alone. Further, air moving down the lee side of the wave warms adiabatically, reducing surface pressures in the lee and adding to the acceleration of winds there.

When the winds aloft are weak or not oriented along the coast, a jet structure (flow at low levels remaining coast parallel and a core of higher winds present) may still occur, as on 9 June south of Cape Blanco. In this case, the lee response appears to be due only to the expansion of the flow rounding Cape Blanco.

A very similar relationship is evident when comparing the flow near Point Sur between the two days. When the winds are strong over Mount Carmel on 9 June (Fig. 17), a deep lee response, oriented along the 850 mb flow, is present in the model. Winds at low levels are quite strong in the lee, and the lateral extent of the lee maximum is quite large. In contrast, winds are relatively weak over Mount Carmel on 14 June (Fig. 18) and the lee response is localized just south of Point Sur.

6. SUMMARY AND CONCLUSIONS

A coastal jet is a persistent feature of the summertime wind pattern along the west coast of the United States. Its position along the coast and the general location of stronger winds within the jet are governed by the position of a ridge extending

to the northeast from the North Pacific high. Increased winds due to the presence of a warm continent are not limited to the boundary layer and inversion.

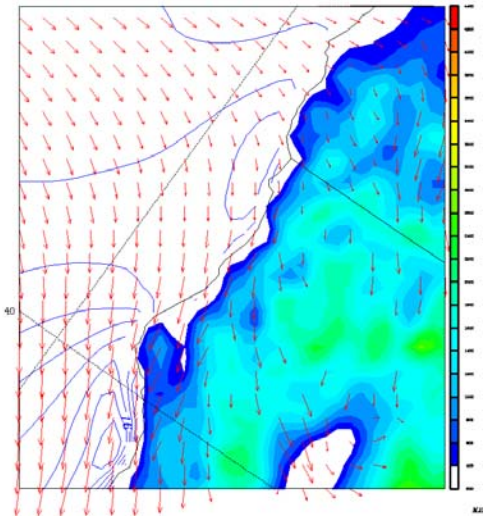

Figure 15. *850 mb wind (arrows, length proportional to speed) and 1000 mb isotachs (2 m s^{-1} contour interval) covering the coast from southern Oregon to northern California, valid at 1900 PDT on 9 June 1996. Terrain shaded at 200-m contour interval above 400 m.*

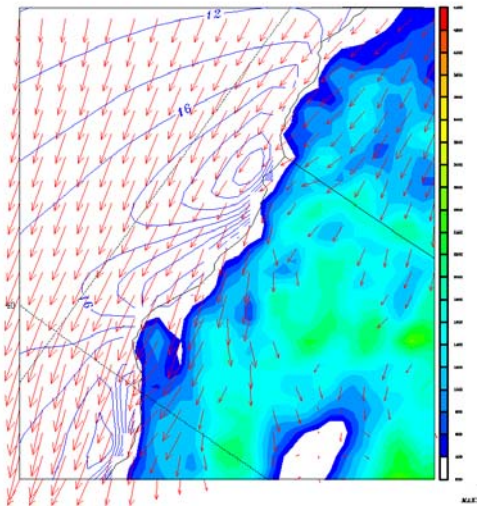

Figure 16. *As in Fig. 15, except from 14 June.*

The coast of southern Oregon and California is characterized by significant topography along most of its length. However, six locations (Chetco Peak, Taylor Peak, Big Mountain area, Santa Cruz Mountains, Mount Carmel (Santa Lucia Mountains), and the Santa Ynez Mountains) are identified with particularly high terrain within 20 km of the coast. Each of these locations induces a characteristic response in the marine boundary

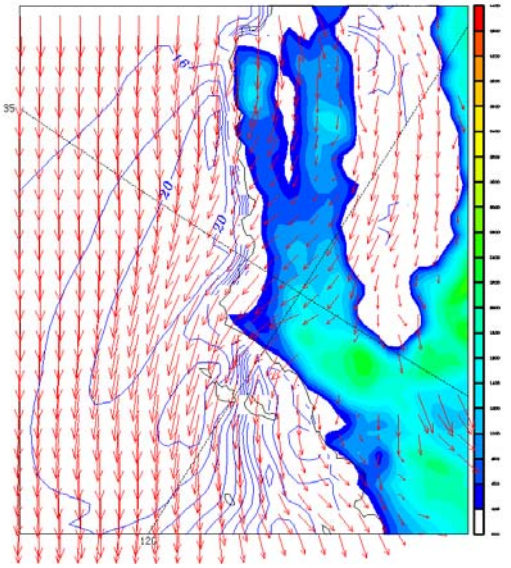

Figure 17. *As in Fig. 15 from 9 June, except for southern portion of study area.*

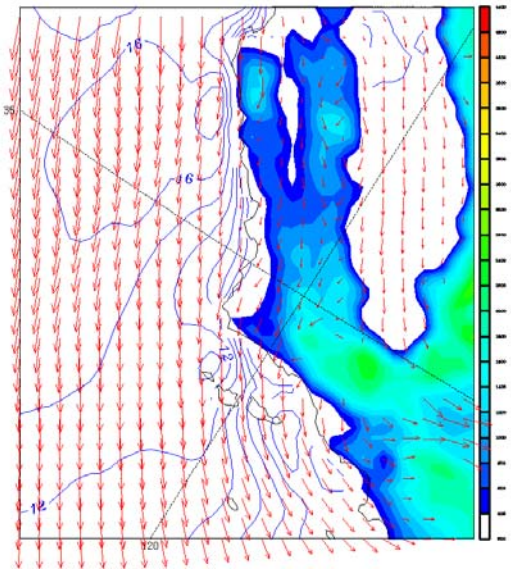

Figure 18. *As in Fig. 17, except from 14 June.*

layer and thus an alteration of the near-shore wind pattern. On the north side of such a feature, the flow within the marine layer is slowed in response to a localized decrease or reversal in the downcoast pressure gradient caused by the combined effects of marine layer deepening, adiabatic cooling of air rising up the terrain, and the higher pressure associated with flow impingement on the upwind side of the mountain. Near the top of the terrain, the flow remains relatively unperturbed until it reaches the mountain top, and is then accelerated down the lee slope, which causes adiabatic warming and a

downstream compression of the marine layer. These effects combine to lower the near-surface pressure, which causes an acceleration of wind in the boundary layer and inversion.

The low-level flow over coastal topography has an offshore extension represented by an area of elevated isentropes and upward deflection in streamlines. Although this flow response decays with distance from the terrain, it can extend to 100 km or more offshore. The compression of the marine layer on the downwind side of these elevations can extend far to the south, accounting for the large size of these features when incident winds are strong.

This isentropic wave pattern over and offshore from significant coastal topography is consistent with mountain wave theory (Cross, 2003). These waves have considerable offshore and downstream extent, and are seen in the model to a distance offshore of approximately one Rossby radius of deformation, at a characteristic angle downstream defined by the supercritical nature of the flow.

Close to shore, the area of lower pressures and shallow marine layer depth downstream of a coastal mountain may be accentuated by the expansion of supercritical flow around an associated coastal bend. On days with weak winds over the coastal mountains, only expansion effects appear to be active, resulting in a reduced-magnitude downstream jet. Both effects cause a lee-side lowering of pressures, shallowing of the marine layer, and increased winds. However, it is the mountain wave that accounts for the large extension of these features offshore and downstream.

The results of this study can be of immediate use for improved forecasts in coastal regions where low-level jets are prevalent. With an understanding of where to expect increased coastal winds with respect to the synoptic 850 mb pattern, combined with an understanding of the nature of the flow interaction with coastal topographic features, a forecaster has the ability to produce a wind forecast of considerable fidelity and skill. That is, given the consistent existence of a coastal jet in summer and the fact that mesoscale structure is driven largely by geographically fixed objects, improved forecasts are possible.

7. REFERENCES

Cross, P.S., 2003: The California coast jet: Synoptic controls and topographically induced mesoscale circulation. Ph.D. Dissertation, Naval Postgraduate School, Monterey, CA, 173 pp.

Durran, D.R., 1986: Mountain waves. *Mesoscale Meteorology and Forecasting*, P.S. Ray, Editor, American Meteorological Society, 472-492.

Hodur, R.M., 1997: The Naval Research Laboratory's coupled ocean/atmosphere mesoscale prediction system (COAMPS). *Monthly Weather Review*, **125**, 1414-1430.

Nuss, W.A., and D.W. Titley, 1994: Use of multiquadric interpolation for meteorological objective analysis. *Monthly Weather Review*, **122**, 1611-1631.

Parish, T.R., 2000: Forcing of the summertime low-level jet along the California coast. *Journal of Applied Meteorology*, **39**, 2421-2433.